Reports

Antarctica: Measuring Glacier Velocity from Satellite Images

B. K. LUCCHITTA AND H. M. FERGUSON

Many Landsat images of Antarctica show distinctive flow and crevasse features in the floating part of ice streams and outlet glaciers immediately below their grounding zones. Some of the features, which move with the glacier or ice stream, remain visible over many years and thus allow time-lapse measurements of ice velocities. Measurements taken from Landsat images of features on Byrd Glacier agree well with detailed ground and aerial observations. The satellite-image technique thus offers a rapid and cost-effective method of obtaining average velocities, to a first order of accuracy, of many ice streams and outlet glaciers near their termini.

MONITORING THE DYNAMICS OF the Greenland and Antarctic ice sheets is an important scientific task because significant changes in the storage of ice within them can severely affect the world's climate and because their disintegration would alter ocean currents and atmospheric temperatures. Furthermore, melting of these two polar ice sheets, which contain more than 90% of the earth's fresh water (*1*), would cause a sea-level rise of as much as 70 m (*2*). Partial melting of the ice sheets may account for the rise in world sea level of more than 5 cm since 1940 (*3*). Yet, it is not known whether the ice sheets are stable, growing, or shrinking, and a thorough and continuing study is of utmost importance. A critical first step in monitoring them and assessing their mass balance is to establish rates of discharge of outlet glaciers that transport ice from the interior of the sheets to the neighboring ice shelves and oceans. The velocities of these rapidly moving glacial masses, including both ice streams (bordered by ice) and glaciers (bordered by rock), constitute one of the two main parameters needed to establish the discharge rate. (The other main parameter, not discussed here, is the area of the cross section of the ice stream or glacier at the point where the average surface velocity was measured.)

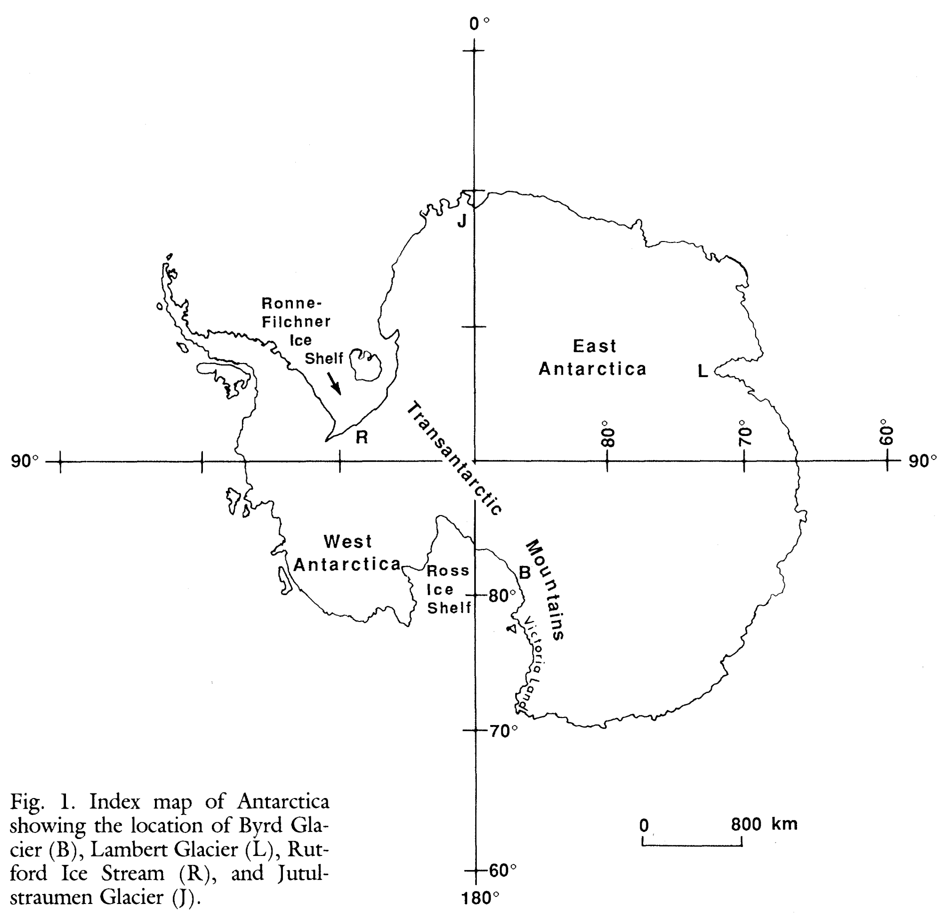

Fig. 1. Index map of Antarctica showing the location of Byrd Glacier (B), Lambert Glacier (L), Rutford Ice Stream (R), and Jutulstraumen Glacier (J).

A rapid and easy method to obtain average velocities of outlet glaciers in Antarctica involves the use of successive Landsat images. During the course of a project to enhance and combine Landsat multispectral scanner (MSS) digital images (resolution, 79 m per picture element) of Antarctica (*4*, *5*), we noticed that many surface features on the lower part of outlet glaciers remain preserved and visible over periods of many years. These features—mainly rifts, depressions, tidal cracks, and crevasses—occur within the floating part of outlet glaciers where they become part of an ice shelf or where they terminate in the ocean. The features are at a developed stage downstream from the grounding zone that separates the sliding and floating parts of the outlet glacier. Tracking these persistent surface features permits measurement of glacier velocity.

To establish the accuracy of measurements of glacier velocity, we investigated successive Landsat images of Byrd Glacier, located in southern Victoria Land (B on Fig. 1), and compared these rates of movement with rates previously established by ground and aerial surveys. This glacier is an ideal test area because it has been studied intensely and was imaged by Landsat in January 1974 and November 1983, an interval of nearly 10 years (Table 1).

Byrd Glacier (Fig. 2) begins as an ice stream behind the Transantarctic mountains in East Antarctica, becomes an outlet glacier flowing east in a fjord through the Transantarctic mountains, and ends as one of many ice streams that form part of Ross Ice Shelf. The glacier is about 25 km wide where it flows through the mountains; it discharges 15 km^3 of ice a year (*6*). Its flow converges into the intake area above the mountains where the glacier spills over a bedrock sill (Figs. 2 and 3), is laminar where the glacier squeezes through the fjord, and diverges where the glacier enters the ice shelf (*6*). Beyond the grounding zone (Fig. 3), where the ice gradually lifts from the bedrock, large transverse crevasses develop. Distinctive structures within this transverse pattern persist for many years, and their displacement can be measured on satellite images.

The origin of this large transverse pattern is not entirely understood. It appears to

U.S. Geological Survey, Flagstaff, AZ 86001.

occur where the ice floats and has divergent flow, and it is seen on the floating part of most large ice streams and glaciers in Antarctica. Examples are Rutford Ice Stream (*7*), Jutulstraumen Glacier (*8*), and Lambert Glacier (Table 1). Hughes (*6*) suggested that tidal flexure may cause transverse crevasse patterns, especially near the grounding zone. Perhaps the large-scale pattern, seen only in synoptic satellite images, reflects the coalescence of many tidal crevasses. Whatever its origin, the slow downstream creep of this transverse pattern permits the measurement of glacier velocity.

Table 1. Landsat images used for this study.

Area	Path/row of Landsat reference grid system	Identification number	Date
Byrd Glacier	46/119	1542-18435	16 January 1974
(80°20′S, 159°00′E)	45/119	40495-18544	23 November 1983
Rutford Ice Stream	225/117	1560-11492	3 February 1974
(79°00′S, 81°00′W)			
Lambert Glacier	135/111	1236-03153	16 March 1973
(71°00′S, 70°00′E)	137/110	1580-03211	23 February 1974
Jutulstraumen Glacier	184/111	2281-07424	30 October 1975
(71°35′S, 0°30′W)	171/111	5034-07520	9 February 1985

For our study of Byrd Glacier, we scaled positive transparencies of two successive Landsat images (Table 1), registered them by reference to identifiable bedrock features, and then measured the movement of distinctive surface patterns in the ice. Precise registration is difficult because of internal distortions within the image frames caused by variations in spacecraft attitude (yaw, pitch, and roll) during image acquisition. Computer processing of images to equivalent scales would solve the registration problem, but it is costly; careful matching of properly scaled images can give adequate results inexpensively and rapidly.

Our measurements indicate that the part of Byrd Glacier downward from the grounding zone moved 7.5 to 8 km in 9 years and 11 months, at an average rate of 750 to 800 m/year (Table 2). Repeated measurements resulted in average errors ranging from 3 to 8%; the low-error values were measured on sharp features, the higher values on more diffuse features. The precision of the method depends on the crispness of the features measured, and only well-defined features lend themselves to measurement.

The rate of 750 to 800 m/year is about the same as those established previously by ground and aerial surveys of the same part of the glacier. Swithinbank (*9*) and Giovinetto *et al.* (*10*) erected a line of survey markers on the ice and established their movement by conventional triangulation from mountains overlooking the ice. They obtained a rate of 740 to 840 m/year. Hughes and Fastook (*11*) monitored the movement of 71 markers on the ice from geodetic ground-control points and additional points established specifically for that monitoring. Their rate was 780 to 820 m/year. Brecher (*12*) identified about 7000 points on the ice in 300 photographs taken by two photographic surveys over a 2-year interval; he measured changed positions with a stereocomparator and established a rate of 740 to 820 m/year. Brecher's points included some on the slower moving ice farther out on the shelf (near points 4 and 5 in Figs. 2 and 3).

These earlier surveys were much more elaborate than ours: they also established

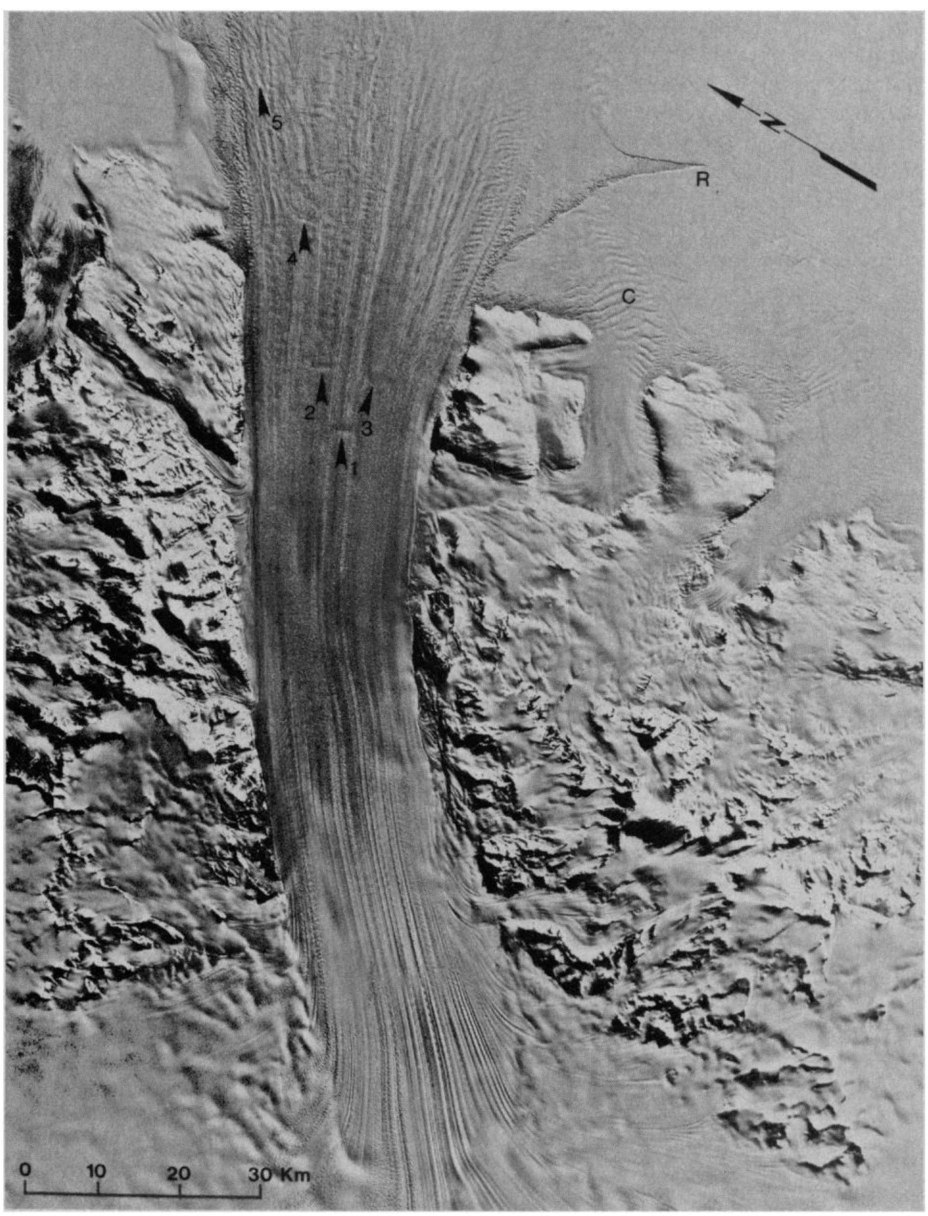

Fig. 2. Byrd Glacier. Transverse rifts whose positions were measured for this report are identified by numbered arrows. Rifts in Couzens Bay are shown at C; large rift at the south side of Byrd Glacier at R. The surface expression of the cirque-like bedrock sill over which the ice stream flows into the fjord is shown at bottom. (Landsat 4 image 40495-18544, 23 November 1983, path 45, row 119.)

velocity profiles across the glacier or velocity contours along it. They were accurate as well: their ground and aerial measurements agree within 3 to 4% (*12*). However, our measurements, made quickly and cheaply, agree with the earlier ones to better than 10%, showing that satellite images may provide the means to monitor ice-stream velocities to a first-order accuracy.

Byrd Glacier is the fastest moving outlet glacier that empties into the Ross Ice Shelf (*9*), and its movements are easily detected. To see if slower movement rates can also be measured on satellite images, we studied displacement of rifts south of Byrd Glacier in Couzens Bay (80°35′S, 160°30′E; point C in Figs. 2 and 3). According to our measurements, the ice moved about 200 m in the 10-year interval (Table 1); the large rift on the south side of Byrd Glacier (point R in Figs. 2 and 3) opened 700 m, and its outer margin drifted about 1.5 km. The data show that displacements can be measured even in slow-moving and smaller glaciers, but the percentage of error increases with decreasing glacier velocity.

For other glaciers and ice streams in Antarctica that were imaged repeatedly by Landsat, identifiable surface features beyond the grounding zone remain visible for a number of years. Images of Lambert Glacier (Table 1), taken only about 1 year apart, show depressions in the glacier (72°S, 68°E) between Fisher Massif (70°29′S, 67°40′E) and Jetty Peninsula (70°30′S, 12°00′E). The depressions moved about 300 m in 341 days, at an average rate of 320 m/year. This rate falls within the range of rates for Lambert Glacier given by Allison (*13*); he measured a rate of 230 m/year 200 km upstream from our point and a rate of 370 m/year 150 km downstream. Our measurements show that, for fast-moving ice, even short time intervals are sufficient to obtain approximate velocities. Jutulstraumen Glacier was also imaged twice (Table 1). Diagnostic structures in its transverse pattern below the grounding zone (*8*) traveled a distance of 7 km in 9 years and 3 months, at an average rate of about 750 m/year.

Satellite images are a valuable tool for certain type of antarctic studies. With them, movement rates of ice streams and glaciers below their grounding zone can be established more quickly and at much lower cost than with the alternative of ground and aircraft surveys. Use of the images makes possible not only compilation of a basic inventory of the rate of flow of outlet glaciers, but also continuous monitoring of changes in velocities.

Hundreds of glaciers discharge ice from the interior of Antarctica, but only a few have been studied in detail and most are

Table 2. Velocities of Byrd Glacier, measured in the floating part below the grounding zone.

Reference	Velocity (m/year)
This report*	
Point 1	780
Point 2	790
Point 3	750
Point 4	750
Point 5	750
Swithinbank (*9*)†	840
Giovinetto *et al.* (*10*)‡	740
Hughes and Fastook (*11*)§	820 to 780
Brecher (*12*)‖	820 to 740

*For location of points, see Figs. 2 and 3. †Extrapolated from table 1 and figure 2 in Swithinbank (*9*); exact location of measured points not given. ‡Given in table 1 of Giovinetto *et al.* (*10*); floating part of glacier. §Extrapolated from figure 3 of Hughes and Fastook (*11*); measured from lower edge of grounding zone to mouth of fjord. ‖Extrapolated from contours in figure 1 of Brecher (*12*); measured from lower edge of grounding zone to vicinity of our measured points 4 and 5 (Figs. 2 and 3).

unexplored. An inventory of their velocities, calculated from successive satellite images, would be a first step in obtaining an estimate of ice discharge. It would also locate the areas where maximum ice discharges are likely to occur, where research efforts should be concentrated in the future, and where continued monitoring of velocities is most critical. Previous monitoring in Antarctica has focused mostly on measuring advances of tidal outlet-glacier termini or ice shelf fronts, which are readily detectable from space (*14–16*).

More than 10 years have passed since the first acquisition of Landsat images of Antarctica. Most early Landsat MSS images of the continent were taken because of the far-sighted efforts of MacDonald (*17, 18*). Since the mid-1970's, coverage by Landsat MSS and thematic mapper images has been sporadic and highly localized. To implement an inventory of ice streams and outlet glaciers, all coastal areas should be reimaged at periodic intervals, preferably at low sun angle to enhance subtle surface morphology.

Landsat images, unfortunately, cover Antarctica to a latitude of only about 81°S; several ice streams and outlet glaciers emptying into the Ross and Ronne-Filchner ice shelves are beyond this imaging limit. Also, cloud-free images of parts of Antarctica within the range of Landsat are not yet available (*19*). Planned satellite imaging-radar systems in polar orbit could fill these

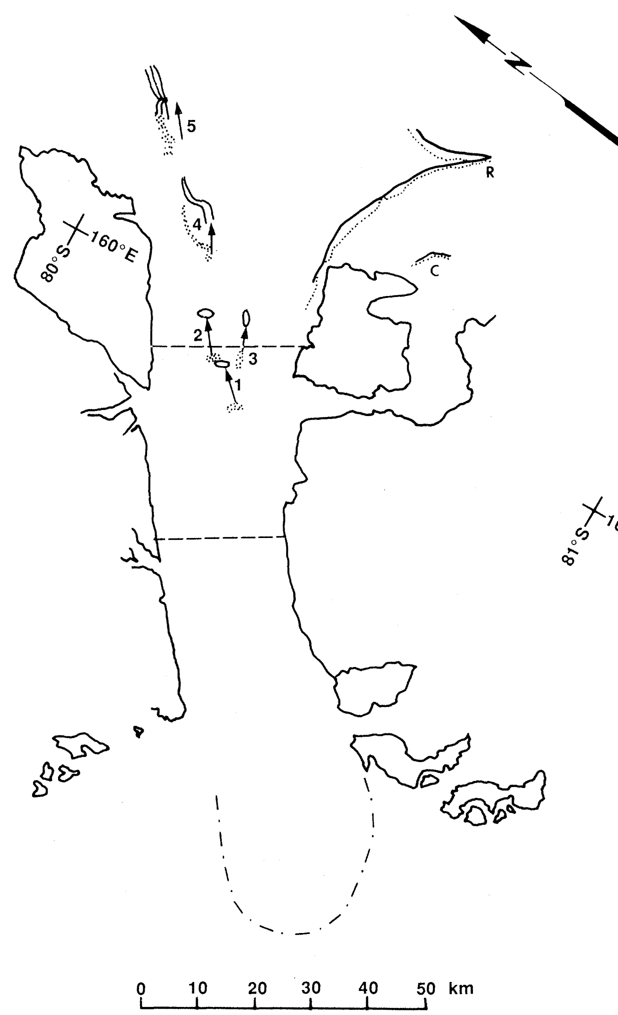

Fig. 3. Sketch map of Byrd Glacier. Dotted areas near the bases of arrows represent the locations of transverse rifts on Byrd Glacier in January 1974; solid lines near heads of arrows show locations of rifts in November 1983. For rates of movement see Table 2. Letters are identical to those used in Fig. 2. Dotted lines near letters show the positions of rifts in Couzens Bay in January 1974; solid lines, their positions in November 1983. Dash-dot line indicates subglacial cirquelike bedrock sill; dashed lines bracket the grounding zone of Hughes and Fastook (*11*).

gaps. They have the capability to image not only through clouds, but also during the darkness of antarctic winters, and they could provide complete coverage in the immediate vicinity of the poles. Several such missions are in the planning stages (*2*).

Overall, the space-borne imaging systems that have now acquired images of Antarctica since the early 1970's, and their successors that will fly repeatedly in the future, offer a unique opportunity to measure the velocity of outlet glaciers and ice streams of the polar ice sheets quickly and inexpensively. These systems will enable us to obtain data that are essential for calculating discharge rates, and, in turn, for monitoring the mass balance of the ice sheets, ultimately helping to monitor associated changes in the world climate.

REFERENCES

1. C. W. M. Swithinbank, *Geogr. Ann. Ser. A* **65**, 289 (1983).
2. R. H. Thomas *et al.*, *NASA Tech. Memo. 86233* (1985).
3. S. D. Hicks, *J. Geophys. Res.* **83**, 1377 (1978).
4. B. K. Lucchitta, E. M. Eliason, C. S. Southworth, *Antarct. J. U.S.* **19**, 249 (1983).
5. B. K. Lucchitta, J. A. Bowell, K. E. Edwards, E. M. Eliason, H. M. Ferguson, *U.S. Geol. Surv. Bull.*, in press.
6. T. Hughes, *Rev. Geophys. Space Phys.* **15**, 1 (1977).
7. C. W. M. Swithinbank and B. K. Lucchitta, *Ann. Glaciol.* **8**, 159 (1986).
8. O. Orheim and B. K. Lucchitta, *ibid.*, in press.
9. C. W. M. Swithinbank, *Science* **141**, 523 (1963).
10. M. Giovinetto, E. S. Robinson, C. W. M. Swithinbank, *J. Glaciol.* **6**, 55 (1964).
11. T. Hughes and J. L. Fastook, *Antarct. J. U.S.* **16**, 86 (1981).
12. H. H. Brecher, *ibid.* **17**, 79 (1982).
13. I. Allison, *J. Glaciol.* **22**, 223 (1979).
14. W. R. MacDonald, *U.S. Geol. Surv. Prof. Pap. 929* (1976), p. 37.
15. R. S. Williams, Jr., J. G. Ferrigno, T. M. Kent, J. R. Schoonmaker, *Ann. Glaciol.* **3**, 321 (1982).
16. D. Lindstrom and D. Tyler, *Antarct. J. U.S.* **19**, 53 (1985).
17. R. B. Southard and W. R. MacDonald, *J. Res. U.S. Geol. Surv.* **2**, 385 (1974).
18. W. R. MacDonald, *U.S. Geol. Surv. Prof. Pap. 929* (1976), p. 194.
19. R. S. Williams, Jr., J. Ferrigno, T. M. Kent, *U.S. Geol. Surv. Open-File Report 84-573*, two sheets, 1:5,000,000 scale map (1984).

16 June 1986; accepted 19 August 1986

Three-Dimensional Structure of Favin: Saccharide Binding–Cyclic Permutation in Leguminous Lectins

GEORGE N. REEKE, JR., AND JOSEPH W. BECKER

The three-dimensional structure of favin, the glucose- and mannose-binding lectin of *Vicia faba* (vetch, broad bean), has been determined at a resolution of 2.8 angstroms by molecular replacement. The crystals contain specifically bound glucose and provide the first high-resolution view of specific saccharide binding in a leguminous lectin. The structure is similar to those of concanavalin A (Con A) and green pea lectin; differences from Con A show that minimal changes are needed to accommodate the cyclic permutation in amino acid sequence between the two molecules. The molecule is an ellipsoidal dimer dominated by extensive β structures. Each protomer contains binding sites for two divalent metal ions (Mn^{2+} and Ca^{2+}) and a specific saccharide. Glucose is bound by favin in a cleft in the molecular surface and has noncovalent contacts primarily with two peptide loops, one of which contains several metal ion ligands. The specific carbohydrate-binding site is similar to that of Con A in location and general peptide folding, despite several differences in specific amino acid residues.

LECTINS INCLUDE A WIDE ASSORTment of proteins from various sources and have the common property of binding specific saccharides (*1, 2*). Although their natural functions are unknown in most cases, and undoubtedly differ among the different classes of lectins, these proteins are highly useful reagents in biochemistry and cell biology. They have been used, among other things, for labeling and studying the dynamics of cell surfaces, for stimulating mitosis in lymphocytes and other cells, and as affinity reagents for isolating glycopeptides and glycoproteins.

Extensive amino acid sequence homologies among the lectins of the Leguminosae suggest a common evolutionary origin for these proteins (*3, 4*). Each of them has protomers of approximately 230 amino acid residues that contain binding sites for Mn^{2+}, Ca^{2+}, and a specific carbohydrate. The protomers can be divided into three subclasses (*5*). The first includes concanavalin A (Con A), the lectin of *Canavalia ensiformis*, which is a tetramer of four identical 237-residue chains. The second includes the glucose- and mannose-binding lectins from *Vicia faba*, *Lens culinaris*, *Pisum sativum*, *Vicia sativa*, and *Vicia cracca*. These proteins are dimers, the subunits of which are composed of an α chain (M_r = 5600) and a β chain (M_r = 20,000), which together are equivalent to a Con A monomer. Comparison of the primary structures of these proteins with Con A reveals an unusual circular permutation of extensive homologous sequences (*6, 7*). In the case of favin, the β chain (residues 1 to 182) homology begins at residue 120 of Con A and extends to the carboxyl terminus of that molecule. It continues without interruption through the amino terminal 69 residues of Con A. The α chain of favin (residues 183 to 233) maintains the continuous homology through the remaining 50 residues (70 to 119) of Con A. The proteins of the third subclass, which includes the lectins from soybeans, peanuts, red kidney beans, and the GalNAc-binding lectins from *V. cracca* and *Dolichos biflorus*, are composed of single chains similar in size to the Con A monomer, but they too are circularly permuted, being equivalent to covalently joined α and β chains of the second subclass. It has been shown recently that these different subclasses arise as a result of different posttranslational modifications of similar precursor molecules which consist of a soybean-type sequence preceded by a signal sequence. In the processing of favin, the signal sequence is removed, a carbohydrate moiety is covalently attached to Asn 168, and the remaining chain is cleaved to produce the mature α and β chains (*8*). The processing of Con A is quite unusual: the signal peptide is removed, the chain is cleaved into smaller chains and then reannealed to produce the circularly permuted sequence expressed in the mature protein (*9*).

Of these lectins, three-dimensional structures have been determined only for Con A (*10–12*) and pea lectin (*13, 14*). Although the saccharide-binding site in Con A has been located by means of heavy atom–labeled carbohydrates at low to medium resolution (*15, 16*), none of the known structures has included bound, unlabeled saccharide at high resolution. We now report the crystallographic determination at a resolution of 2.8 Å of the structure of favin. This study allows us to compare the chain foldings of permuted sequences from two different subclasses. In addition, crystals of favin were grown in the presence of glucose, providing the first opportunity to examine the specific carbohydrate-protein binding interactions of a leguminous lectin at high resolution.

The asymmetric unit of favin crystals (*17*) contains a complete dimeric molecule (M_r = 51,000) comprising two α chains, two β

Department of Developmental and Molecular Biology, Rockefeller University, New York, NY 10021.